Water-Related Adsorbates on Stepped Platinum Surfaces

Kolb, Manuel Jerome

Chapter 1

Introduction

1.1 Fossil fuels, Renewable Energies and Electrochemistry

Fossil fuels are finite. This fact, as un-surprising as it is, will have a large influence on our daily lives already during the lifespan of the current generation. The increase in the cost of energy, be it gas or electricity and the increase in cost of oil-related products will influence our decision-making in the years to come. This makes approaches to reduce our reliance on oil and natural gas for the simple use as energy carriers a key aspect of current scientific research. One of the very few feasible possibilities to overcome this problem is the use of renewable energy sources such as wind, geothermal, solar and water power.

However, many renewable energy sources also currently have massive drawbacks. Germany as one of the most prominent examples for production of renewable energy currently experiences these deficiencies. Figure 1.1 shows the electrical power production of Germany for the first week of January 2015 (Figure 1.1a) and the first week of June 2015 (Figure 1.1b). As can be seen clearly, solar and wind power are, from a technical standpoint, far from ideal candidates for the production of the majority of a country's electricity because of the large variance in their hourly and monthly energy generation rates. An additional challenge is the physical transport of the energy generated, where the energy loss during transmission via power lines increases with geographical distance between the places of production and consumption. Many ideas exist on how to create solutions for the storage problem, one of the oldest being pumped hydro storage powerplants. However, these solutions also have issues, due to their large ecological impact on the environment in which they are built and their limited storage capacities. Also, as discussed above, being able to transport the stored energy

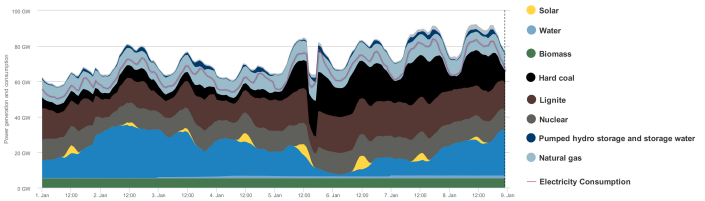

(a) German electrical power production in the first week of January 2015

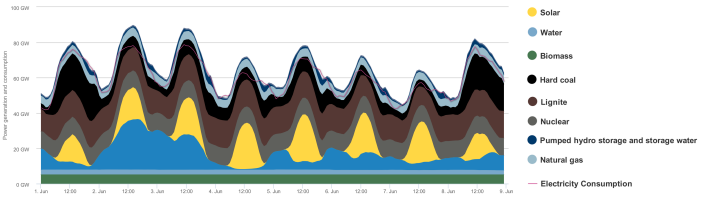

(b) German electrical power production in the first week of June 2015

Figure 1.1: German electrical power production in the first week of January and June 2015. Data points are given each hour, and separated by different energy sources. Taken from [1]

in a physical medium would help alleviate the transfer problems as well as allow for the use of these energy carriers as mobile fuels for e.g. cars. Electrochemistry offers many approaches for the use of electricity to store energy. The most common of these are the use of batteries and the related supercapacitors for the direct storage of electricity, and the use of electrolysis and fuel cells for the production and conversion of energy carriers. Possible energy carriers are hydrogen via the hydrogen evolution reaction (HER) or also hydrocarbons generated by the reaction of hydrogen with CO_2, which can then also be transported physically, helping to alleviate the transportation problem. The benchmark catalyst for the HER is the platinum surface. However, platinum is not the metal of choice for large-scale industrial applications due to its high price and low availability. This means that either different catalysts need to be found that can produce similar reaction rates, while still offering a competitive price for the catalyst, or the efficiency of the available platinum must be optimized.

1.2 Linking Surface Science and DFT to Electrochemistry

The search for new catalysts or the desire to make better use of the existing ones requires a detailed understanding of the underlying chemical and physical properties of the platinum surface. Its interaction with the solvent, the electrolyte, the reactant, intermediates and product, and the co-adsorption properties of all of these will influence the reactivity. Additionally, the behavior of water at room temperature, the pH level and the applied voltage will also influence the reaction mechanism. All of these properties must be fully understood to arrive at a complete set of requirements for an improved catalyst. Unfortunately, due to the strong interconnection of all of these properties, elucidating them completely in the real electrochemical environment is not easily feasible. Therefore, approaches that allow for the separation of smaller subsets of these from the electrochemical environment are needed.

Two main approaches are capable of this task: Theoretical approaches, such as density functional theory (DFT) can provide binding energies and models for the interaction of the solvent with the species on the surface, as well as provide information on reaction pathways and onset potentials of the reactions. Unfortunately, these models are limited in their predictive power, both due to their accuracy, as well as due to limitations in the modeling process. Ultra-high-vacuum surface science on the other hand allows for an experimental measurement of physical properties, such as desorption temperatures and sticking probabilities (which are linked to the adsorption energy and barrier), as well as reaction rates for surface-catalyzed reactions. However, also this technique has a downside, which is characterized as the "pressure gap". One of the main differences in this regard, is of course the absence of the full solvent environment under UHV conditions. The solvent can influence the chemical reaction in many ways. First, the solvent molecules can adsorb on the catalyst surface, thereby creating competitive adsorption between the solvent and the reactant. Second, the solvent molecules, when co-adsorbed, can interact favorably or unfavorably with the reactants, intermediates and products which can promote or hinder the chemical reaction. Third, the solvent can act as a reactant itself, by for example acting as a hydrogen donor for an electrochemical hydrogenation step. Consequently, a UHV study is conducted under significantly different environmental conditions than the related electrochemical experiment, which might lead to different behavior of the real system due to the difference in its surroundings.

This means that none of the methods described above by itself can provide a full and meaningful picture of an electrochemical reaction, but by interconnecting

all of the results from all of the techniques there is a good chance to arrive at a more complete picture.

1.3 Defective Surfaces

Due to the difficulty in describing the full chemical reaction in a realistic catalytic system, which generally consists of nano-particles on a support, usually high-symmetry facets of the catalytic metal are chosen as model systems. The well-ordered nature of these facets helps significantly in the elucidation of the chemical processes happening on the surface. The reason for this is that due to the reduced number of distinct adsorption geometries, the identification of the reactive sites and their behavior during the reaction can be deduced from the experimental and theoretical data. Due to the large number of different sites present on nano-particles, this is generally not possible for the real system. Unfortunately, the high-symmetry facets sometimes do not provide a complete picture, since low-coordinated adsorption sites can contribute significantly to the total reaction rates[2, 3].

Due to this, approaches are needed to study low-coordinated lattice sites in the context of surface science and theoretical chemistry[2]. The most common of these approaches is the use of regularly stepped surfaces. These surfaces consist of flat high-symmetry facets that are interrupted by single-atom-high step edges at periodic intervals. The periodicity of the intervals can be chosen very accurately in the experiment by cutting a single-crystal surface slightly outside the chosen high-symmetry plane. The resulting regularly-stepped surface can now be used to identify the experimental behavior of the low-coordinated lattice sites. This is done by separating the results into properties attributed to the high-symmetry terraces and the step-edge sites.

With very few exceptions this experimental approach works very well and has given rise to a general understanding of the reactive behavior of step edges. However, arriving at a detailed microscopic understanding often requires additional data. This can be provided by theoretical approaches, such as density functional theory (DFT).

1.4 Density Functional Theory

The investigation of a multi-atom system at an *ab initio* level requires finding the solution to the Schrödinger equation, which contains a significant number of degrees of freedom. Density Functional Theory makes use of several simplifications to achieve this, which will be briefly discussed in the following [4].

The full Hamiltonian of a system containing atomic cores and electrons is described by:

$$\hat{H} = \hat{T}_e + \hat{T}_c + \hat{V}_{ee} + \hat{V}_{cc} + \hat{V}_{ec} + \hat{V}_{ext}, \tag{1.1}$$

where $\hat{T}_e$ and $\hat{T}_c$ are the kinetic energies of the cores and electrons, $\hat{V}_{ee}$ and $\hat{V}_{cc}$ are the interaction potentials of the particles of the same kind and $\hat{V}_{ec}$ denotes the interaction potential between electrons and cores. $\hat{V}_{ext}$ denotes any external potential acting on the system.

Considering the mass differences between the electrons and cores, it is generally assumed that the electronic part of the Hamiltonian reacts almost instantaneously to changes in the coordinates of the cores. This allows for the separation of the Hamiltonian into an electronic part and a part for the nuclei, which can be treated separately. This separation is called the Born-Oppenheimer approximation:

$$\hat{H}_e = \hat{T}_e + \hat{V}_{ee} + \hat{V}_{ec} + \hat{V}_{ext,e} \tag{1.2}$$

$$\hat{H}_c = \hat{T}_c + \hat{V}_{cc} + \hat{V}_{ext,c} + E_e^0, \tag{1.3}$$

where $\hat{V}_{ext,e}$ and $\hat{V}_{ext,c}$ describe any external potential acting on the electrons or cores and E_e^0 denotes the total energy of the electronic system at a given set of core coordinates. The part containing the cores can now be treated with classical mechanics, while the simplified electronic part needs to be treated with quantum-mechanical methods.

In 1964 Hohenberg and Kohn [5] described a method to calculate the ground state of the wave function of a solid solely based on its electron density $n(\mathbf{r})$, which allows for the reduction of the complexity of the full electronic system with its $3 \cdot N$ coordinates to a system with only 3 coordinates, where N is the number of electrons in the system. Building on this scheme, one year later Kohn and Sham [6] showed that the Hohenberg-Kohn functional can also be written as:

$$\left(\hat{T} + V_H[n] + V_{XC}[n] + V_{ext,e}[n]\right) \phi_i = \epsilon_i \phi_i. \tag{1.4}$$

In this equation, $\hat{T}$ denotes the kinetic energy operator, $V_H[n]$ is the Hartree potential, which describes the electrostatic interaction between the electrons, $V_{XC}[n]$ is the exchange correlation potential and $V_{ext,e}[n]$ describes any external field acting on the electrons. ϕ_i are single-electron wave functions of a auxiliary non-interacting system, where

$$n(\mathbf{r}) = \sum_i^N f_i |\phi_i|^2. \tag{1.5}$$

Unfortunately, this approach cannot reduce the actual complexity inherent in the description of the system, but only shifts it into the exchange-correlation

part of the equation. For this part no closed expression can be calculated for any extended system since this problem has the same complexity as solving the Schrödinger equation for the system itself. However, as it turns out, relatively simple approximations for the exchange correlation energy, such as the local density approximation (LDA) or the generalized gradient approximation (GGA) can provide surprisingly accurate results given their rather simple nature. The GGA approach is built upon the work by Perdew and Wang [7], in which they propose an approximation for the exchange correlation energy that is not only based upon the local density (as is the LDA functional) but also on the gradient of the local density.

$$E_{XC}[n] = \int \epsilon_{XC}\left(n, |\nabla n|\right) \cdot n \; d^3r. \tag{1.6}$$

In this work, the PBE functional, proposed by Perdew, Burke and Ernzerhof [8] is used for the approximation of $E_{XC}[n]$. It was chosen for its universally good representation of adsorption energies for all the systems that were considered[9–11]. A more detailed justification for the use of this functional can be found in the relevant sections detailing the theoretical methods for chapters 2 and 3.

1.5 Review of Previous Experimental and Theoretical Results

In this thesis we will discuss the interaction of water-related adsorbates with stepped platinum surfaces, namely the Pt(533) surface and the Pt(553) surface. The choice of adsorbates was made in order to arrive at a more detailed understanding of previously obtained UHV data from our group, as well as to arrive at a better understanding of the interaction of the electrochemical environment with the step edges of platinum surfaces. The two model surfaces consist of a 4-atom-wide terrace and a one-atom-high step for Pt(533) and a 5-atom-wide terrace and a one-atom-high step for Pt(533) and were chosen to mirror the surfaces studied in the experiments. In the following we will discuss the current state of research for the adsorbates that are discussed in this thesis: hydrogen, oxygen, OH and water.

1.5.1 Hydrogen

The adsorption of hydrogen has been the focus of multiple experimental studies due to its link to hydrogenation reactions in heterogenous catalysis, as well as the hydrogen evolution reaction in electrocatalysis. In UHV temperature programmed desorption (TPD) experiments it was found that on Pt(111) hydrogen

displays a single-peak desorption spectrum around $\sim$ 300 K [12]. Introducing a high density of single-atom-high steps gives rise to additional adsorption peaks: for the Pt(211)[13] and Pt(533)[14–16] surface a single high-temperature peak appears at around 370 K on both surfaces. This peak is assigned to the desorption from the (100)-type step edges present on these surfaces, and an increased binding energy is assumed for these sites. The Pt(553)[14] surface shows a significantly more complex spectrum with 2 additional peaks at temperatures below 300 K. This was interpreted by assigning the peak at 300 K to the Pt(111) terrace, while the lowest temperature peak was assigned to the desorption from the (111)-type step edge. Surfaces with increased geometric complexity, such as the Pt(110)-(2x1) missing row reconstruction were also studied with the TPD method and also a spectrum with 3 peaks was identified [17]. The origin of these peaks was however not clear.

DFT simulations of hydrogen adsorption on Pt(111) [18] found a very flat energy landscape for the adsorption wells for low-coverage hydrogen adsorption on the infinite (111) terrace. In a later publication Olsen et al. also discussed the adsorption of low-coverage hydrogen on the regularly stepped Pt(211) surface, which contains (100)-type step edges[19]. It was found that the bridging position at the top of the step edge shows a significantly enhanced binding energy for this step-edge type. In order to elucidate the previously unexplained TPD spectrum of the Pt(110)-(2x1) reconstructed surface Gudmundsdóttir et al. performed high-coverage hydrogen adsorption simulations[20, 21]. It was found that the desorption barriers which are present on this surface significantly alter the order of the desorption pathways compared to what the pure adsorption energies would suggest.

1.5.2 Oxygen

The desorption of oxygen from Pt(111) was studied by Gland et al. [22] using temperature programmed desorption. It was found that oxygen shows two desorption features: a low-temperature feature that was assigned to molecular oxygen trapped in a shallow well above the surface and a high-temperature peak that stems from chemically adsorbed atomic oxygen that associatively desorbs. Adsorption of oxygen at various coverages on the stepped Pt(533) and Pt(553) surfaces was performed in our group [14]. It was found that oxygen exhibits a three peak spectrum for both surfaces: a low temperature peak for the molecular adsorption well, a medium-temperature peak stemming from the (111) terrace and a high-temperature peak originating from the step edges. Note that the desorption temperatures for the step desorption differ between the two surfaces, with Pt(553) exhibiting a lower desorption temperature for the step edge than Pt(533).

Oxygen adsorption on stepped surfaces was also studied using DFT. Feibelmann et al. [23] investigated the adsorption of oxygen on the stepped Pt(211) and Pt(221) surfaces. It was found that oxygen prefers the bridged binding site on the Pt(211) surface, while at the (111)-type step oxygen sits in the FCC site adjacent to the upper step edge.

1.5.3 OH

Under UHV conditions water does not split into OH and H [24] on flat or stepped platinum surfaces. This is in contrast to the case in electrochemical conditions, where the presence of OH on the terrace of stepped surfaces is confirmed and the presence of OH on the step edge is strongly suspected[25]. This disparity stems from the differences in the surrounding environment, namely temperature, pressure and the presence of additional water, protons, OH and the applied potential. These factors allow the water to split into OH and H under electrochemical conditions, while under UHV conditions overcoming the energy difference inherent to the reaction is not possible. However, the coadsorption of atomic oxygen with water can allow for the formation of OH on the step and the terrace of Pt(533)[24, 26] under UHV conditions. In both cases it was observed that the OH is preferentially formed at the terraces for full oxygen coverages. OH is more strongly bound at step sites for both surfaces, however it is assumed that the terrace-bound OH inhibits the formation of step-bound OH.

The adsorption of OH has been studied extensively with DFT. On Pt(111) the half-dissociated water layer as it can be encountered in the electrochemical environment was discussed [27, 28] in detail, due to its link to the oxygen reduction reaction (ORR). The half-dissociated water layer consists of a stable $(\sqrt{3} \times \sqrt{3})$-overlayer, in which every second water molecule is dissociated to form OH. The question whether water will split into OH and H at the step edges that occur on a Pt(111) surface were also a concern for theoretical investigations. The most recent examples are the investigations by Donadio et al. and Peköz et al. for the Pt(221) surface [10, 29], in which they find that the dissociation is not favored for single water molecules. The presence of additional water molecules will facilitate the dissociation by incorporating the formed OH into a hydrogen-bonded network.

1.5.4 H_2O

The interaction of water with the surface of platinum has been the subject of numerous experimental studies [30–35]. On the Pt(111) surface two main adsorption structures have been recorded: a $(\sqrt{37} \times \sqrt{37})$ structure at coverages below one monolayer and a $\sqrt{39} \times \sqrt{39}$ structure that is dominant at coverages

of 1 ML. The structures that are observed do not only contain the hexagonal pattern present in crystalline hexagonal ice I_h, but also pentagons and heptagons. Regularly stepped surfaces were studied with TPD in our group [14], where it was found that water exhibits a two peak spectrum on the Pt(533) and Pt(553) surfaces. The desorption temperatures are very similar for both step-types. The high-temperature peak that only appears on these stepped surfaces is interpreted as strongly bound water adsorbed on the step edges. Additionally, the step edges on defective Pt(111) surfaces were studied using scanning tunneling microscopy (STM) by Morgenstern et al. [32], who observed that the two step edge types present on these surfaces exhibit significantly differing adsorption behavior.

Water adsorption structures have also been discussed in the context of DFT studies. For the Pt(111) surface the $\sqrt{37} \times \sqrt{37}$ and $\sqrt{39} \times \sqrt{39}$ [30] adsorption structures were both verified using DFT calculations. Additional consideration was given to the interaction between the aqueous environment and a fully hydrogen-covered Pt(111) surface, where it was found that the hydrogen layer passivates the surface and leads to a reduced interaction between the water and the surface [36]. Water adsorption on regularly stepped platinum surfaces was first discussed by Meng et al [37], where they proposed the formation of a 1 one-dimensional line structure along the step edge. Additional studies on this topic were performed later by Arnadottir et al. [38, 39].

1.6 Outline of the thesis

The subsequent chapters of the thesis are ordered in the following way:

In chapter 2 we focus on the low-coverage adsorption regime on both model surfaces. We study the adsorption of hydrogen, oxygen, OH and water across the complete surface and arrive at a detailed understanding of the adsorption site preferences. Furthermore, we show that for the Pt(533) surface the low-coverage picture is sufficient to arrive at a clear understanding of the experimental TPD spectra, while for the Pt(553) surface, only water and oxygen can be explained fully by this approach. For the hydrogen desorption from the Pt(553) surface we can only explain the low-coverage part of the spectrum, while a full picture for the the high-coverage part remains elusive. Additionally, we use our data to calculate energetics for the autocatalytic splitting of water at the step-edge sites.

In chapter 3 we model high-coverage water adsorption structures on the (100)-type step edge of Pt(533). We gradually increase the coverage beyond the low-coverage regime and arrive at adsorption geometries of water for medium and high coverage. We find that water forms two lines along the upper and lower step edge, which can be connected in a large number of ways to form different ring

sizes. We find multiple structures with very similar adsorption energies with ring sizes ranging from 4 (tetragons) to 7 (heptagons).

In chapter 4 we present a combined STM and DFT project that investigates the adsorption structures of water around the (111) step edge of Pt(553). We performed a similar DFT analysis for the adsorption geometries as presented on the Pt(533) surface and find that the (111)-type edge present on Pt(553) strongly prefers the formation of double-stranded tetragonally-linked water structures. Our experimental collaborators confirm the formation of these double-stranded water networks on the surfaces using low-temperature scanning tunneling microscopy (STM).

In chapter 5 we discuss high-coverage hydrogen-adsorption calculations on both model surfaces. This is done to help elucidate the previously not well-understood TPD spectrum originating from the Pt(553) surface. On Pt(533) we find that the adsorption energies fall into two main energy ranges, which correspond to the two peaks visible in the TPD spectrum. On Pt(553) we identify the step-edge site as the most favorable adsorption site. Combining this with the experimentally-obtained ratio of the integrals of the different peaks allows us to arrive at a value for the maximum coverage on this surface. It is found that this coverage is significantly lower than on Pt(533). The low-temperature part of the spectrum is found to originate from two energetically different sites on the middle of the terrace of the surface.

The short chapter 6 gives a short summary on the supporting information for each chapter. The subsequent chapter 7 gives a short outlook on possible follow-up projects, while the final chapter 8 gives conclusions based on the obtained results.

References

(1) Energiewende, A. Agorameter., Retrieved on 26.11.2015, `http://www.agora-energiewende.de/en/topics/-agothem-/Produkt/produkt/76/Agorameter/`.

(2) Marković, N. M.; Ross, P. N. *Surf. Sci. Rep.* **2002**, *45*, 117 –229.

(3) Koper, M. T. M. *Nanoscale* **2011**, *3*, 2040–3364.

(4) Dreizler, R. M.; Gross, E. K., *Density Functional Theory: An Approach to the Quantum Many-Body Problem*; Springer: Berlin, Apr. 1996.

(5) Hohenberg, P.; Kohn, W. *Phys. Rev.* **1964**, *136*, B864–B871.

(6) Kohn, W.; Sham, L. J. *Phys. Rev.* **1965**, *140*, A1133–A1138.

(7) Perdew, J. P.; Yue, W. *Phys. Rev. B* **1986**, *33*, 8800–8802.

(8) Perdew, J. P.; Burke, K.; Ernzerhof, M. *Phys. Rev. Lett.* **1996**, *77*, 3865–3868.

(9) Vasić, D.; Ristanović, Z.; Pašti, I.; Mentus, S. English *Russian Journal of Physical Chemistry A* **2011**, *85*, 2373–2379.

(10) Peköz, R.; Wörner, S.; Ghiringhelli, L. M.; Donadio, D. *The Journal of Physical Chemistry C* **2014**, *118*, 29990–29998.

(11) Carrasco, J.; Klimeš, J.; Michaelides, A. *The Journal of Chemical Physics* **2013**, *138*, 024708.

(12) Christmann, K; Ertl, G; Pignet, T *Surface Science* **1976**, *54*, 365 –392.

(13) Badan, C.; Koper, M. T. M.; Juurlink, L. B. F. *The Journal of Physical Chemistry C* **2015**, *119*, 13551–13560.

(14) Van der Niet, M. J. T. C.; den Dunnen, A.; Juurlink, L. B. F.; Koper, M. T. M. *J. Chem. Phys.* **2010**, *132*, 174705.

(15) Gee, A. T.; Hayden, B. E.; Mormiche, C.; Nunney, T. S. *The Journal of Chemical Physics* **2000**, *112*, 7660–7668.

(16) Gee, A.; Hayden, B.; Mormiche, C; Nunney, T. *Surface Science* **2002**, *512*, 165 –172.

(17) Kirsten, E.; Parschau, G.; Stocker, W.; Rieder, K. *Surface Science* **1990**, *231*, L183 –L188.

(18) Olsen, R. A.; Kroes, G. J.; Baerends, E. J. *The Journal of Chemical Physics* **1999**, *111*.

(19) Olsen, R.; Badescu, S.; Ying, S.; Baerends, E. *J. Chem. Phys.* **2004**, *120*, 11852–11863.

(20) Gudmundsdóttir, S.; Skúlason, E.; Jónsson, H. *Phys. Rev. Lett.* **2012**, *108*, 156101.

(21) Gudmundsdottir, S.; Skulason, E.; Weststrate, K.-J.; Juurlink, L.; Jonsson, H. *Phys. Chem. Chem. Phys.* **2013**, *15*, 6323–6332.

(22) Gland, J. L.; Sexton, B. A.; Fisher, G. B. *Surface Science* **1980**, *95*, 587 –602.

(23) Feibelman, P. J.; Esch, S.; Michely, T. *Phys. Rev. Lett.* **1996**, *77*, 2257–2260.

(24) Van der Niet, M. J. T. C.; Berg, O. T.; Juurlink, L. B. F.; Koper, M. T. M. *The Journal of Physical Chemistry C* **2010**, *114*, 18953–18960.

(25) Van der Niet, M. J. T. C.; Garcia-Araez, N.; Hernández, J.; Feliu, J. M.; Koper, M. T. M. *Catalysis Today* **2013**, *202*, 105 –113.

(26) Van der Niet, M. J. T. C.; den Dunnen, A.; Juurlink, L. B. F.; Koper, M. T. M. *Phys. Chem. Chem. Phys.* **2011**, *13*, 1629–1638.

(27) Tripković, V.; Skúlason, E.; Siahrostami, S.; Nørskov, J. K.; Rossmeisl, J. *Electrochimica Acta* **2010**, *55*, 7975 –7981.

(28) Lew, W.; Crowe, M. C.; Campbell, C. T.; Carrasco, J.; Michaelides, A. *The Journal of Physical Chemistry C* **2011**, *115*, 23008–23012.

(29) Donadio, D.; Ghiringhelli, L. M.; Delle Site, L. *Journal of the American Chemical Society* **2012**, *134*, 19217–19222.

(30) Feibelman, P. J.; Bartelt, N. C.; Nie, S.; Thrmer, K. *The Journal of Chemical Physics* **2010**, *133* 154703.

(31) Fisher, G. B.; Gland, J. L. *Surface Science* **1980**, *94*, 446 –455.

(32) Morgenstern, M.; Michely, T.; Comsa, G. *Phys. Rev. Lett.* **1996**, *77*, 703–706.

(33) Nie, S.; Feibelman, P. J.; Bartelt, N. C.; Thürmer, K. *Phys. Rev. Lett.* **2010**, *105*, 026102.

(34) Zimbitas, G.; Haq, S.; Hodgson, A. *The Journal of Chemical Physics* **2005**, *123* 174701, –.

(35) Zimbitas, G.; Hodgson, A. *Chemical Physics Letters* **2006**, *417*, 1 –5.

(36) Roman, T.; Groß, A. *Catalysis Today* **2013**, *202*, 183 –190.

(37) Meng, S.; Wang, E. G.; Gao, S. *Phys. Rev. B* **2004**, *69*, 195404.

(38) Arnadottir, L.; Stuve, E. M.; Jonsson, H. *Surf. Sci.* **2010**, *604*, 1978 –1986.

(39) Arnadottir, L.; Stuve, E. M.; Jonsson, H. *Surface Science* **2012**, *606*, 233 –238.